Kalman Filter Based Newton Extremum Seeking Control for Maximum Gases Production Rates of Anaerobic Digestion Process

Yang Tian, Maobo Hu, Haoping Wang

LaFCAS Laboratory, Automation School, Nanjing University of Science and Technology, 200 Xiao Ling Wei St, 210094 Nanjing, China

Ivan Simeonov, Lyudmila Kabaivanova

The Stephan Angeloff Institute of Microbiology – Bulgarian Academy of Sciences, Acad. G. Bonchev St, bl. 26, 1113 Sofia, Bulgaria

Nicolai Christov

LaFCAS Laboratory, CRISTAL Research Center, Lille University, 59655 Villeneuve d'Ascq, France

Corresponding author: hp.wang@njust.edu.cn

This paper proposes a Kalman filter (KF) based Newton extremum seeking control (NESC) to maximize production rates of hydrogen and methane in anaerobic digestion process. The Kalman filtering algorithm is used to obtain more accurate gradient and Hessian estimates which makes it possible to increase the convergence speed to the extremum and to eliminate input and output steady-state oscillations. The simulation examples demonstrate the performances of the proposed approach.

KEYWORDS: Anaerobic digestion process, Kalman filter, Extremum seeking control.

1. Introduction

Anaerobic digestion (AD) gets more and more attention nowadays because it is a relatively cheap, sustainable and efficient method to treat organic wastes. AD makes possible to realize depollution of organic wastes for environment protection, production of energy in the form of biogas (including hydrogen and methane) and creation of biofuels 16.

The anaerobic digestion of organic wastes is a very complex multi-stage biochemical process which involves the interaction between the metabolic processes of many different microorganisms and complex organic matter transformations affected by a variety of environmental factors. Microbial activity during AD is a crucial feature for process stability and biogas yield, and thus requires further investigation 1. The AD process mathematical models are characterized by nonlinearities and parametric and/or model uncertainties. Most mathematical models of AD processes are based on mass-balance equations or on a zonal description of the bioprocess variables (model with variable structure) 8. At present, AD models are mainly divided into two categories. The first one consists of complex models, such as ADM1 (Anaerobic Digestion Model 1) 6 using 35 state equations to describe the AD process in detail. The other one includes simplified or reduced-order models which mainly describe some special chemical and biochemical phenomena. From control point of view, these simplified models are convenient for control applications. The most representative ones are Droop model 11, Andrews model 3 and Bernard model 7.

In order to obtain good performances and high quality production, various control and observer algorithms have been developed and used for AD process control: sliding mode observer based optimal control 3, non-parametric adaptive control 25, and robust nonlinear observer 17. Moreover, artificial intelligence control strategies such as neural networks 4, fuzzy control 12 and multi-model observe based estimator 22, have been applied to AD processes. In the past ten years, model free controllers 29 have also been developed for AD processes. Because prior information for the AD process is usually unknown or limited, different estimators and/or observers are used for plant coefficients estimation and/or state observation in these controllers.

The extremum seeking control (ESC) is a classic method for system performance optimization requiring generally only input and output system information [19, 28]. Recently, a number of important ESC development results have been published, such as multi-input ESC 5, sliding mode ESC 24, time-varying ESC 15, Newton based ESC 21, fractional order ESC 2, etc.

In this paper, a KF based NESC is proposed to optimize an AD system for hydrogen and methane production in order to obtain maximum gas production rates. The AD system consists of a cascade of two continuously stirred anaerobic bioreactors which can produce hydrogen and methane separately. In this AD system, hydrogen can't be detected as it is consumed immediately by hydrogenotrophic methanogens to produce methane (CH_4) and carbon dioxide (CO_2) 14. By dividing the AD process into two stages of hydrogen production and methanogenesis, the considered AD system can completely utilize the organic acids produced during dark fermentation and improve the overall energy conversion efficiency [9, 23].

The proposed KF based NESC algorithm do not require any process model information and uses only input and output measurements – dilution rate and the biogas outflow rate. The gradient and Hessian of the static input-output map are estimated using Kalman filter, which makes it possible to speed up the convergence to the extremum. Moreover, there are no steady-state oscillations because the amplitude of the perturbation signal converges to zero during steady state regime. This ensures the smoothness of the dilution rate and the gas production rate.

The paper is organized as follows. In Section 2, the anaerobic digestion process model and the optimization criterions are described. The KF based NESC is presented in Section 3. Numerical simulation results are presented and discussed in Section 4, and some concluding remarks are given in Section 5.

2. Model of Anaerobic Digestion Process

The AD process can be divided in four main phases of hydrolysis, acidogenesis, acetogenesis and methanogenesis. In the hydrolysis phase, undissolved complex

organic compounds are hydrolyzed into small molecule compounds. In the acidogenesis stage, small molecule compounds are converted to volatile fatty acids (VFAs), hydrogen and carbon dioxide. In the acetogenesis phase, some VFAs (propionate and butirate) are decomposed into acetate, hydrogen and carbon dioxide. In the methanogenesis phase, the acetoclastic methanogenic bacteria transform the acetate into methane and carbon dioxide.

In the two-stage AD system illustrated in Figure 1, relatively fast growing acidogens and H_2 producing microorganisms are developed in the first-stage hydrogenic bioreactor (BR1) which encompasses the first two phases of AD process:

$$S_0^{in} \longrightarrow S_0$$
$$S_0 \xrightarrow{X_1} S_1 + H_2 + VFAs, \tag{1}$$
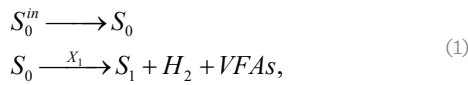
where S_0^{in}, S_0 and S_1 are the concentrations of the inlet organic wastes, macromolecular organics and soluble small molecule organics, and X_1 is the acidogenic bacteria concentration.

On the other hand, the slow growing acetogens and methanogens are developed in the second-stage methanogenic bioreactor (BR2), which contains the last three phases:

$$Pr_2 \xrightarrow{X_{Pr}} AC_2$$
$$But_2 \xrightarrow{X_{But}} AC_2 \tag{2}$$
$$AC_2 \xrightarrow{X_{Ac}} CH_4,$$
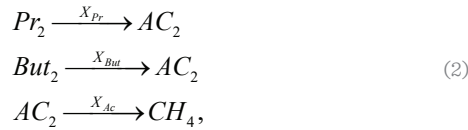
where Pr_2, But_2 and AC_2 are propionate, butirate and acetate concentrations, and X_{Pr}, X_{But} and X_{Ac} denote, respectively, propionic acid-degrading bacteria, butyric acid-degrading bacteria and methanogenic bacteria concentrations.

As we can see three intermediate products: acetate, propionate and butyrate produced in the BR1 will flow into BR2, where propionate and butyrate are further converted to acetate and after that to CH_4 and CO_2.

These biochemical reactions lead to a mathematical model of a cascade of two continuously stirred anaerobic bioreactors. The model of BR1 and BR2 is established by the principle of mass balance. The models can be expressed by the following Equation (Equation (3.a) is the model of BR1, Equation (3.b) is the model of BR2) 9 :

Figure 1

AD process with production of hydrogen and methane
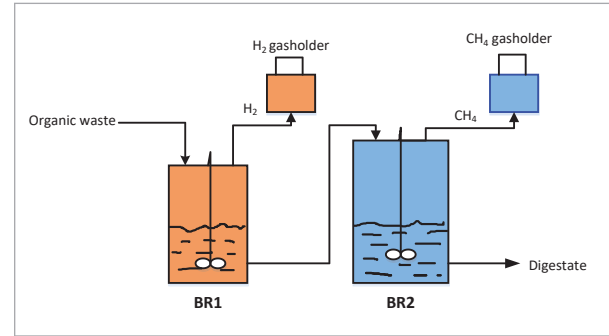
$$\frac{dS_1}{dt} = -D_1 S_1 + \beta X_1 S_0 + \frac{\mu_1 X_1}{Y_1}$$

$$\frac{dX_1}{dt} = \mu_1 X_1 - D_1 X_1$$

$$\frac{dPr_1}{dt} = \frac{\mu_1 X_1}{Y_{Pr1}} - D_1 Pr_1$$

$$\frac{dBut_1}{dt} = \frac{\mu_1 X_1}{Y_{But1}} - D_1 But_1 \tag{3a}$$

$$\frac{dAc_1}{dt} = \frac{\mu_1 X_1}{Y_{Ac1}} - D_1 Ac_1$$

$$Q_{H_2} = Y_{H_2} \mu_1 X_1$$

$$\frac{dX_{Pr}}{dt} = \mu_{Pr} X_{Pr} - D_2 X_{Pr}$$

$$\frac{dPr_2}{dt} = -\frac{\mu_{Pr} X_{Pr}}{Y_{Pr2}} + D_2 (Pr_1 - Pr_2)$$

$$\frac{dX_{But}}{dt} = \mu_{But} X_{But} - D_2 X_{But}$$

$$\frac{dBut_2}{dt} = -\frac{\mu_{But} X_{But}}{Y_{But2}} + D_2 (But_1 - But_2) \tag{3b}$$

$$\frac{dX_{Ac}}{dt} = \mu_{Ac} X_{Ac} - D_2 X_{Ac}$$

$$\frac{dAc_2}{dt} = -\frac{\mu_{Ac} X_{Ac}}{Y_{Ac2}} + \frac{\mu_{Pr} X_{Pr}}{Y_{Pr2}} + \frac{\mu_{But} X_{But}}{Y_{But2}}$$
$$+ D_2 (Ac_1 - Ac_2)$$

$$Q_{CH_4} = Y_{CH_4} \mu_{Ac} X_{Ac},$$

where μ_1, μ_{Pr}, μ_{But}, μ_{Ac} denote, respectively, the Mono-type growth rate of acidogenic bacteria, propi-

onic acid-degrading bacteria, butyric acid-degrading bacteria and methanogenic bacteria; Y_p, Y_{But1}, Y_{H_2}, Y_1 are yield coefficients; Q_{H_2}, Q_{CH_4} represent the hydrogen and methane production rate, and β is a constant parameter. The dilution ratios D_1 and D_2 of BR1 and BR2 have the following relationship:

$$\frac{D_1}{D_2} = K, \tag{4}$$

where the coefficient K is related with the ratio of the working volumes of both bioreactors 9. The anaerobic digestion model parameters values are given in Table 1.

Table 1

The model parameters

μ_{1max}	0.568	maximum specific growth rate of acidogenic bacteria (h^{-1})
μ_{Prmax}	0.05	maximum specific growth rate of propionate degrading bacteria (h^{-1})
μ_{Butmax}	0.05	maximum specific growth rate of butyrate degrading bacteria (h^{-1})
μ_{Acmax}	0.025	maximum specific growth rate of methanogenic bacteria (h^{-1})
K_{s_1}	3.914	saturation coefficient for acidogenic bacteria (g/dm^3)
K_{Pr}	0.22	saturation coefficient for propionate (g/dm^3)
K_{But}	0.22	saturation coefficient for butyrate (g/dm^3)
K_{Ac}	0.8	saturation coefficient for acetate (g/dm^3)
β	1	coefficient of biodegradability (g.h)
Y_p	1	coefficient (-)
Y_1	0.08	yield coefficient for acidogenic bacteria (-)
Y_{Pr1}	4.2	yield coefficient for propionate (-)
Y_{But1}	2.1	yield coefficient for butyrate (-)
Y_{Ac1}	1.1	yield coefficient for acetate (-)
Y_{Pr2}	1.5	yield coefficient for propionate (-)
Y_{But2}	1.5	yield coefficient for butyrate (-)
Y_{Ac2}	0.5	yield coefficient for acetate (-)
Y_{H_2}	0.22	yield coefficient for hydrogen (dm^3/g)
Y_{CH_4}	142	yield coefficient for methane (dm^3/g)

The objective of controlling the anaerobic digestion process is to maximize the hydrogen production rate Q_{H_2} and total gas production rate $Q=Q_{H_2}+Q_{CH_4}$. The AD system presented above has a distinct optimum in the input-output static characteristic maps (D_1 and Q_{H_2}, D_1 and Q), see Figures 2-3. It is obvious that the more the concentration of waste organics S_0^{in} is added, the more the concentration of the corresponding substrate which can be used by bacteria (in the admissible range without inhibition), and eventually the gases outflow rates are increased.

Figure 2
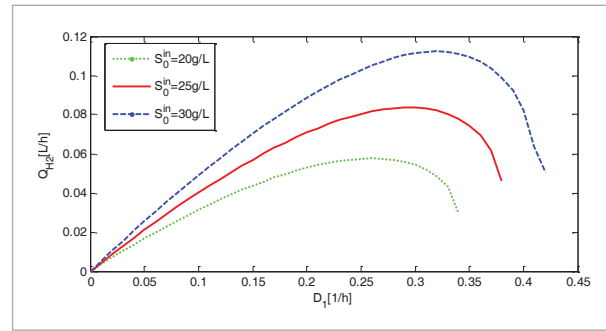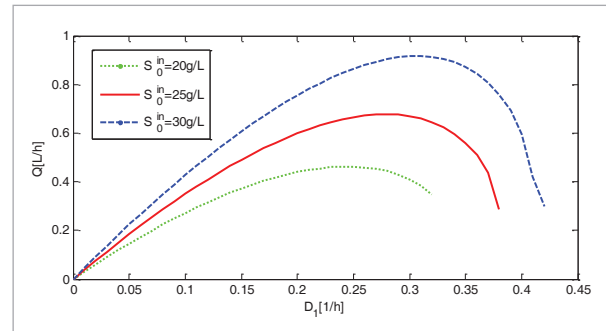
Static characteristic D_1-Q_{H_2} for different S_0^{in}

Figure 3

Static characteristic D_1-Q for different S_0^{in}


3. KF Based Newton Extremum Seeking Control

In this section, a KF based NESC is designed to stabilize dilution rate D_1 while maximizing the hydrogen production rate Q_{H_2} and gases production rate Q. The corresponding schematic diagram of the proposed KF based NESC is shown in Figure 4. The

proposed method can regulate the input θ as close as possible to θ^* when only the output and optimization target of the system are available and no or partly system information is known.

The AD system input θ is obtained by superimposing the perturbation signal p to the estimate $\hat{\theta}$ of θ, produced by the Newton optimizer. The KF based estimator uses the output and input of the AD system to estimate in real time the gradient $\hat{b}$ and Hessian $\hat{H}$ of the input-output static map $y = f(\theta)$. The estimates $\hat{b}$ and $\hat{H}$ are then used by the Newton optimizer in order to obtain $\hat{\theta}$ which moves toward θ^*.

Figure 4

Structure of the Kalman filter based Newton extremum seeking control
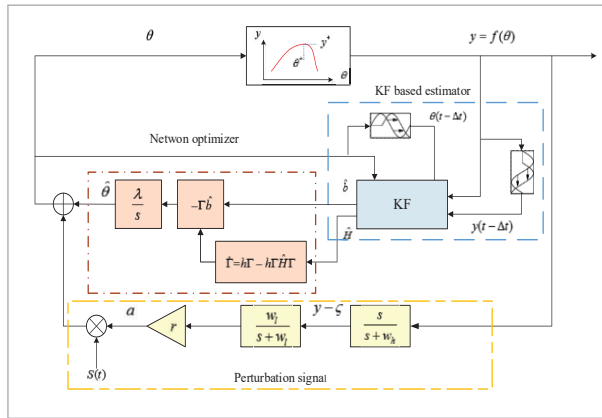
3.1. AD System

The considered AD system (3) can be written in the standard state-space form

$$\begin{cases} \dot{x} = \varphi(x, u) \\ y = \psi(x) \end{cases},$$ (5)

where $x \in R^n$ is the system state (the concentration of various organic acids and bacteria), $u \in R$ is the input, $y \in R$ is the output (Q_{H_2}, Q_{CH_4} or Q), and $\varphi : R^n \times R \to R^n$ and $\psi : R^n \to R$ are smooth functions. Suppose that there exists a smooth control law

$$u = \alpha(x, \theta)$$ (6)

parameterized by a scalar parameter θ, for which the closed-loop system has a unique equilibrium. In particular, we can select the dilution rate D_l as the input u, and u can be considered as θ in the AD system.

The input-output static function of the AD system $y = f(\theta)$ has an extremum point (θ^*, y^*), where y^* is the maximum value of the system output.

3.2. Newton Optimizer

In this paper, the estimate $\hat{\theta}$ is computed by the Newton-based optimization algorithm 20

$$\frac{d\hat{\theta}}{dt} = -k\Gamma\hat{b}$$ (7)

$$\frac{d\Gamma}{dt} = h\Gamma - h\Gamma^2\hat{H}$$ (8)

until reaching the extremum point. Here k, h >0 are design parameters, $\hat{b}$ and $\hat{H}$ are the estimates of the gradient and the second derivative (the Hessian) of the AD input-output static function $y = f(\theta)$, and Γ is the estimate of the inverse of the Hessian H. The Riccati Equation (8) has two equilibrium points: $\Gamma^* = 0$ and $\Gamma^* = \hat{H}^{-1}$. Because $h > 0$, the equilibrium point $\Gamma^* = 0$ is unstable and the equilibrium point $\Gamma^* = \hat{H}^{-1}$ is exponentially stable. Thus Γ converges to the actual value of H^{-1} if $\hat{H}$ is a good estimate of the Hessian H. In addition, by adjusting the value of parameter h, the convergence speed of the control algorithm can be adjusted to a certain extent.

3.3. KF Based Estimator

The estimation of the gradient and Hessian of the unknown static input-output function $y = f(\theta)$ is a key element of NESC 18. In the proposed ESC, a Kalman filter [13, 30] is used to replace the linear filter based estimator used in the classical ESC scheme [21, 28]. The use of KF makes possible to obtain faster and more accurate gradient and Hessian estimation, which can speed up the convergence of the algorithm. More details on the real-time state estimation by KF can be found in [26, 30].

The function $y = f(\theta)$ can be approximated as follows:

$$f(\theta) = f(\overline{\theta}) + b(\theta - \overline{\theta}) + \frac{H}{2}(\theta - \overline{\theta})^2 + o(\theta - \overline{\theta})$$
$$\Rightarrow \Delta f = b\Delta\theta + \frac{1}{2}H\Delta\theta^2,$$ (9)

where $\Delta f = f(\theta) - f(\overline{\theta})$, $\Delta\theta = \theta - \overline{\theta}$. The unknown gradient b and Hessian H define the states of the Kal-

man filter: $x_1 = b$ and $x_2 = H$. It is assumed that these states are constant. Discrete Kalman filter is implemented using the state and measurement equations

$$x(t_{k+1}) = \begin{bmatrix} x_1(t_{k+1}) \\ x_2(t_{k+1}) \end{bmatrix} = \underbrace{\begin{pmatrix} 1 & 0 \\ 0 & 1 \end{pmatrix}}_{F} x(t_k) + \omega_k$$

$$z(t_k) = \begin{bmatrix} \Delta y(t_k) \\ \Delta y(t_{k-n}) \end{bmatrix}$$

$$= \underbrace{\begin{bmatrix} \Delta\theta(t_k) & \frac{1}{2}\Delta\theta(t_k)^2 \\ \Delta\theta(t_{k-n}) & \frac{1}{2}\Delta\theta(t_{k-n})^2 \end{bmatrix}}_{M_k} x(t_k) + \upsilon_k,$$

(10)

where $\Delta y(t_k) = y(t_k) - y(t_{k-1})$, $\Delta y(t_{k-n}) = y(t_{k-n}) - y(t_{k-n-1})$, $\Delta\theta(t_k) = \theta(t_k) - \theta(t_{k-1})$, $\Delta\theta(t_{k-n}) = \theta(t_{k-n}) - \theta(t_{k-n-1})$, and ω_k, υ_k are independent normally distributed white noises with covariance matrices Q and R, respectively. The time-shifted input-output pair $(\Delta\theta(t_{k-n}), \Delta y(t_{k-n}))$ is used to ensure the system observability.

The estimates $\hat{b}$ and $\hat{H}$ of b and H are calculated by the following Kalman filter algorithm27:

$$\hat{x}_k^- = F x_{k-1}$$
$$P_k^- = F P_{k-1} F^T + Q$$
$$K_k = P_k^- M_k^T R^{-1}$$
$$\hat{x}_k = x_k^- + K_k(z_k - M_k x_k^-)$$
$$P_k = (P_k^{-1} + M_k^T R^{-1} M_k)^{-1},$$

(11)

where $\hat{x}_k^-$ is the prior state estimate at the k-th step when the state x_{k-1} is known, $\hat{x}_{k-1}$ and $\hat{x}_k$ are the state estimates at the k-th and k-1 steps, P_k^- and P_k are the prior error covariance matrix and covariance matrix at step k, and K_k is the Kalman gain at step k.

3.4. Perturbation Signal

To ensure the feasibility of the gradient and Hessian estimation in real time, a perturbation signal is superimposed on the Newton optimizer output $\hat{\theta}$. In this paper the perturbation signal $aS(t)$ is used, where

$$a = r\frac{w_l}{s + w_l}(y - \zeta), \quad \zeta = \frac{s}{s + w_h}y$$

(12)

$$S(t) = \sin(\eta(t)), \quad \eta(t) = w\pi(1 + \sin W(t)),$$

(13)

Here w_l and w_h are the cutoff frequencies of the cor-

responding low-pass high-pass filters, $r > 0$ is a constant gain for adjusting the convergence speed, $W(t)$ is the standard Brownian motion process, and w is a positive constant.

When the system output y converges to its maximum value y^*, the amplitude of the perturbation signal approaches to zero, which makes possible to eliminate the steady-state oscillations.

4. Simulation Results

We can see that the input-output static characteristics $Q_{H_2} = Q_{H_2}(D_1)$ of BR1 and $Q = Q(D_1)$ of the AD system from Figure 2 - 3. With hydrogen production rate Q_{H_2} and total gases production rate Q as optimization targets, KF based NESC is applied to the AD system to demonstrate its effectiveness. It is supposed that:

1 Only the dilution rate D_1 and the production rate of hydrogen Q_{H_2} or total gas Q are available for online measurement.

2 The inlet organics concentration S_0^{in} is constant (load disturbance), and the simulation experiments are carried out under the condition of $S_0^{in} = 25$g/L.

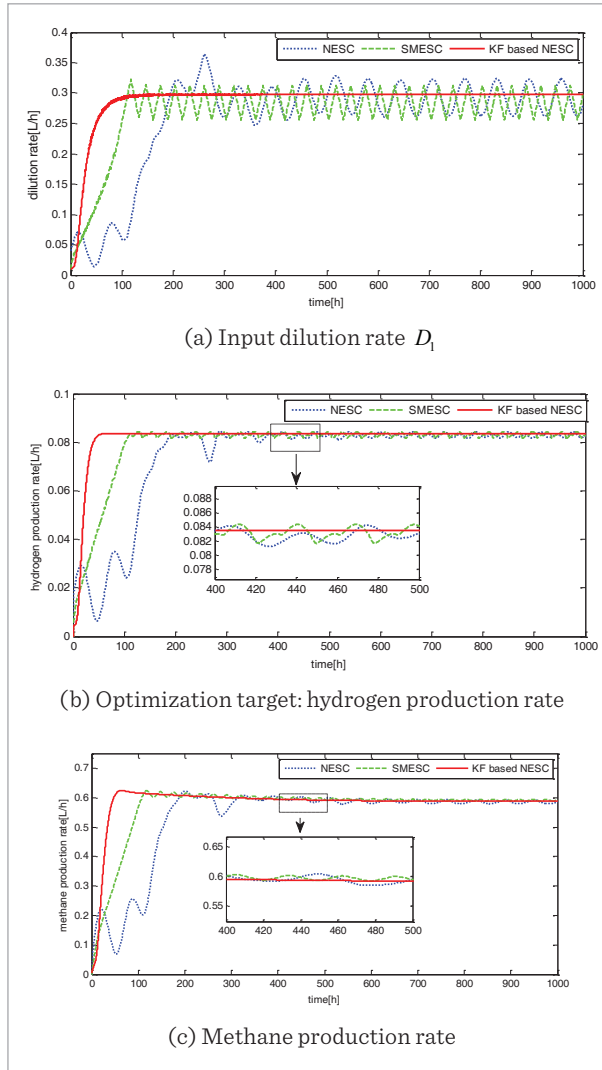### 4.1. Maximizing Hydrogen Production Rate

The AD process optimization is achieved by controlling the dilution rate of BR1 in order to maximize the hydrogen production rate. To demonstrate the performances of the proposed KF based NESC, they are compared with the performances of the sliding mode ESC (SMESC) 24 and Newton ESC (NESC) 21. In order to ensure that KF based NESC has better control performance, the parameters in the control algorithm are set as: $k = 0.0045$, $r = 0.1$, $w_l = 0.02$, $w_h = 0.08$, $w = 0.1$ rad/s, $\Gamma(0) = -0.06$. The SMESC design parameters are $k = 0.004$ and $\beta = 0.0007$. In turn, the NESC design parameters are $k = 2$, $w_l = 0.02$, $w_h = 0.08$, $w = 0.1$ rad/s and $\Gamma(0) = -0.06$.

The comparison between the three controllers for initial dilution rate $D_1(0) = 0.01\ h^{-1}$ is shown in Figure 5. Furthermore, the trajectories of the operating point for different initial values of the dilution rate ($D_1(0) = 0.01, 0.15, 0.25, 0.35\ h^{-1}$) are given in Figure 6.

It can be seen that for the three ESC, the hydrogen production rate converges to a maximum value of
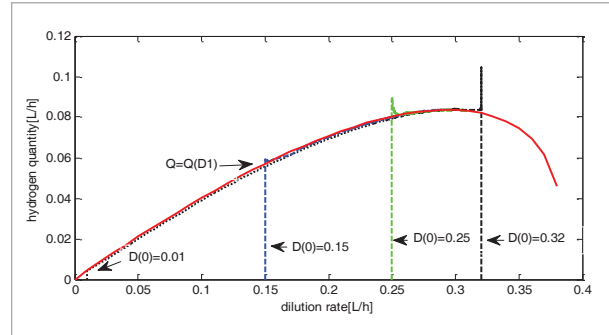
Figure 5

AD processes for hydrogen production rate as optimization target

(a) Input dilution rate D_i

(b) Optimization target: hydrogen production rate

(c) Methane production rate

Figure 6

The trajectories of the operating point in the plan for different initial values of the dilution rate under KF based NESC
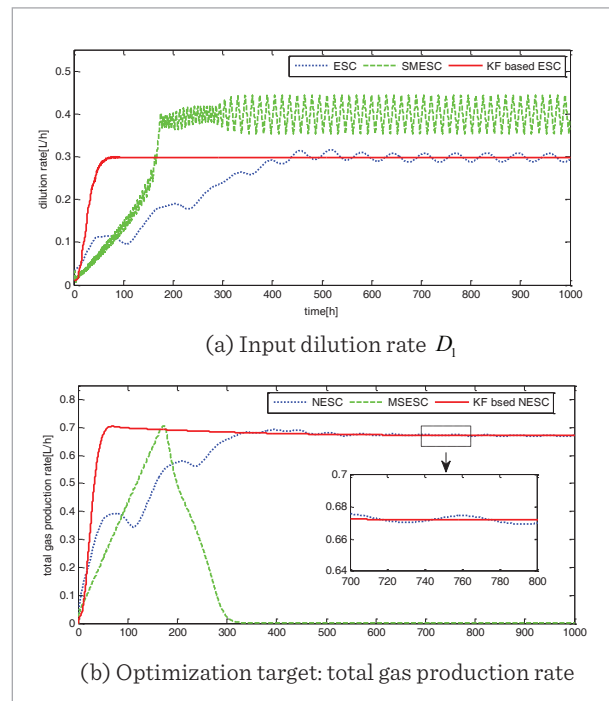

4.2. Maximizing Total Gas Production Rate

In this subsection, the total gas production rate Q is considered as optimization target. Figure 7 shows the simulation results with similar parameters as in the previous subsection except $k = 0.0048$ in KF based NESC, $k = 1.6$ in NESC, and $k = 0.012$, $\beta = 0.004$ in SMESC.

Figure 7

AD processes for hydrogen production rate as optimization target

(a) Input dilution rate D_i

(b) Optimization target: total gas production rate

about 0.083 L/h, and the methane production rate is also the same (about 0.58 L/h). However, in terms of convergence time, the proposed KF based NESC is the fastest, followed by SMESC, and the Newton ESC is the slowest. Compared with the other two ESCs, the biggest advantage of the ESC scheme proposed in this paper is the smoothness of the dilution rate and the gas production rate, which is advantageous for the actuators that control the dilution rate and gas collectors. As it is illustrated in Figure 6, the robustness of the control with respect to different initial values of $D_i(0)$ is satisfactory for the KF based NESC.

It can be seen that the proposed KF based NESC ensures faster convergence to the maximum of the total gas production rate (about 0.67 L/h) than the NESC, while the closed-loop system with SMESC can not find the optimal dilution rate (about 0.29 1/h).

5. Conclusion

This paper deals with the extremum seeking control of cascade of two continuously stirred anaerobic bioreactors which can produce simultaneously both biohydrogen and biomethane. The mixed gas produced from both bioreactors, known as hythane, provides a higher heating value as compared to that obtained from a single-stage anaerobic process.

In order to achieve maximum gases production rates (maximum energy), a new extremum seeking control - Kalman filter based Newton extremum seeking control - is proposed making possible to optimize the system performances by measuring only the process input and output. The Kalman filter is used to obtain more accurate gradient and Hessian estimates, which makes it possible to speed up the convergence to the extremum, and to avoid steady-state oscillations. The performances of the proposed extremum seeking control are studied by numerical simulations and compared with those of standard Newton ESC and sliding mode ESC. The obtained results show the higher performances of the new extremum seeking control.

Rererences

1. Ahring, B. K., Ahring, B. K., Angelidaki, I, Dolfing, J., Stamatelatou, K. Biomethanation II. Advances in Biochemical Engineering biotechnology, 2003, 82. http://dx.doi.org/10. 1007/3-540-45838-7

2. Ammar, N., Ladaci, S., Charef, A., Loiseau, J. Fractional Order Extremum Seeking Approach for Maximum Power Point Tracking of Photovoltaic Panels. Frontiers in Energy, 2015, 9(1), 43-53. https://doi.org/10.1007/s11708-014-0343-5

3. Andrews, J. F., Pearson, E. A. Kinetics and Characteristics of Volatile Acid Production in Anaerobic Fermentation Processes. Air & Water Pollution, 1965, 9, 439-461. http://dx.doi.org /10. 1080/01944 366608978498

4. Antwi, P., Li, J., Boadi, P. O., Meng, J., Shi, E., Deng, K., Bondinuba, F. K. Estimation of Biogas and Methane Yields in an UASB Treating Potato Starch Processing Wastewater with Backpropagation Artificial Neural Network. Bioresource Technology, 2017, 228, 106-115. https://doi.org/10.1016/j.biortech.2016.12.045

5. Ariyur, K. B., Krstić, M. Analysis and Design of Multivariable Extremum Seeking. Proceedings of the American Control Conference, 2002, 4, 2903-2908. https://doi.org/10.1109/ACC.2002.1025231

6. Batstone, D. J., Keller, J., Angelidaki I, Kalyuzhnyi, S. V., Pavlostathis, S. G., Rozzi, A., Sanders, W. T. M, Siegrist, H., Vavilin, V. A. The IWA Anaerobic Digestion Model No 1 (ADM1). Water Science and Technology, 2002, 45(10), 65-73. https://doi.org/10.2166/wst.2002.0292

7. Bernard, O., Hadj-Sadok, Z., Dochain, D., Genovesi, A., Steyer, J. P. Dynamical Model Development and Parameter Identification for an Anaerobic Wastewater Treatment Process. Biotechnology & Bioengineering, 75(4), 424-438. https://doi.org/10.1002/bit.10036

8. Caraman, S., Ifrim, G., Ceangă, E., Barbu, M., Titica, M., Precup, R. E. Extremum Seeking Control for an Anaerobic Digestion Process. In 2015 19th International Conference on System Theory, Control and Computing (ICSTCC), 2015, 243-248. https://doi.org/10.1109/ICSTCC.2015.7321300

9. Chorukova, E., Simeonov, I. Mathematical Modeling of the Anaerobic Digestion in Two-Stage System with Production of Hydrogen and Methane Including Three Intermediate Products. International Journal of Hydrogen Energy, 2019. https://doi.org/10.1016/j. ijhydene.2019.01.228

10. Daaou, B., Dochain, D. Sliding Mode Observer Based Real-Time Optimization of Production Rate in a Bioreactor. 2017 IEEE 56th Annual Conference on Decision and Control, CDC 2017, 2018, 2108-2113. https://doi.org/10.1109/CDC.2017.8263958

11. Droop, M. R. The Kinetics of Uptake Growth and Inhibition in Monochrysis Lutheri. Journal of Marine Biology, 1968, 48, 680-733. https://doi.org/10.1017/S0025315400019238

12. Estaben, M., Polit, M., Steyer, J. P. Fuzzy Control for an Anaerobic Digester. Control Engineering Practice, 1997, 5(9), 1303-1310. https://doi.org/10.1016/S0967-0661(97)84369-9

13. Gelbert, G., Moeck, J. P., Paschereit, C. O., King, R. Advanced Algorithms for Gradient Estimation in One- and Two-Parameter Extremum Seeking Controllers. Journal of Process Control, 2012, 22(4), 700-709. https://doi.org/10.1016/j.jprocont.2012.01.022

14. Gerardi, M. H. The Microbiology of Anaerobic Digesters. John Wiley & Sons, 2003. https://doi.org/10.1002/0471468967.ch7

15. Guay, M., Dochain, D. A Time-Varying Extremum-Seeking Control Approach. Automatica, 2015, 51, 356-363. https://doi.org/10.1016/j.automatica.2014.10.078

16. Lakov, V., Simeonov, I. Comparative Study of Algorithms for Extremum Seeking Control for Extremum Seeking Control of Organic Waste Anaerobic Digestion Process. International Conference Automatics and Information, 2017.

17. Lara-Cisneros, G., Aguilar-López, R., Dochain, D., Femat, R. On-line Estimation of VFA Concentration in Anaerobic Digestion via Methane Outflow Rate Measurements. Computers and Chemical Engineering, 2016, 94, 250-256. https://doi.org/10.1016/j.compchemeng.2016.07.005

18. Kebir, A., Woodward, L., Akhrif, O. Extremum-Seeking Control With Adaptive Excitation: Application to a Photovoltaic System. IEEE Transactions on Industrial Electronics, 2018, 65(3), 2507-2517. https://doi.org/10.1109/TIE.2017.2745448

19. Krstić, M., Wang, H. H. Stability of Extremum Seeking Feedback for General Nonlinear Dynamic Systems. Automatica, 2000, 36(4), 595-601. https://doi.org/10.1016/S0005-1098(99)00183-1

20. Liu, S. J., Krstic, M. Newton-Based Stochastic Extremum Seeking. Automatica, 2014, 50(3), 952-961. https://doi.org/10.1016/j.automatica.2013.12.023

21. Moase, W. H., Manzie, C., Brear, M. J. Newton-Like Extremum-Seeking for the Control of Thermoacoustic Instability. IEEE Transactions on Automatic Control, 2010, 55(9), 2094-2105. https://doi.org/10.1109/TAC.2010.2042981

22. Morel, E., Tartakovsky, B., Guiot, S. R., Perrier, M. Design of a Multi-Model Observer-Based Estimator for Anaerobic Reactor Monitoring. Computers and Chemical Engineering, 2006, 1(2), 78-85. https://doi.org/10.1016/j.compchemeng.2006.05.003

23. Pakarinen, O. M., Kaparaju, P. L. N., Rintala, J. A. Hydrogen and Methane Yields of Untreated, Water-Extracted and Acid (HCl) Treated Maize in One- and Two-Stage Batch Assays. International Journal of Hydrogen Energy, 2011, 36(22), 14401-14407. https://doi.org/10.1016/j.ijhydene.2011.08.028

24. Pan, Y., Özgüner, Ü., Acarman, T. Stability and Performance Improvement of Extremum Seeking Control with Sliding Mode. International Journal of Control, 2003, 6(9-10), 968-985. https://doi.org/10.1080/0020717031000099100

25. Petre, E., Selişteanu, D., Şendrescu, D. Adaptive and Robust-Adaptive Control Strategies for Anaerobic Wastewater Treatment Bioprocesses. Chemical Engineering Journal, 2013, 17, 363-378. https://doi.org/10.1016/j.cej.2012.11.129

26. Simon, D. Optimal State Estimation - Kalman, H∞, and Nonlinear Approaches. John Wiley & Sons, Inc. 2006. https://doi.org/10.1002/0470045345.ch7

27. Speyer, J. L., Chung, W. H. Stochastic Processes, Estimation, and Control. Advances in Design and Control. SIAM, first edition, 2008. https://doi.org/10.1137/1.9780898718591

28. Wang, H. H., Krstić, M. Extremum Seeking for Limit Cycle Minimization. IEEE Transactions on Automatic Control, 2000, 5(12), 2432-2436. https://doi.org/10.1109/9.895589

29. Wang, H. P., Tian, Y., Kalchev, B., Simeonov, I., Christov, N. Pilot-scale Biogas Plant: Description, Modelling and Composed Recursive Control. Control Engineering and Applied Informatics, 2013, 15(2), 38-45. https://doi.org/10.1109/ MCS. 2013.2249411

30. Ye, M., Hu, G. A Robust Extremum Seeking Scheme for Dynamic Systems with Uncertainties and Disturbances. Automatica, 2016, 66, 172-178. https://doi.org/10.1016/j.automatica.2015.12.034